FORMATION OF CLAY MINERALS DURING LOW TEMPERATURE EXPERIMENTAL ALTERATION OF OBSIDIAN

MOTOHARU KAWANO,[1] KATSUTOSHI TOMITA,[2] AND YOSHITAKA KAMINO[3]

[1] Department of Environmental Sciences and Technology, Faculty of Agriculture
Kagoshima University, 1-21-24 Korimoto, Kagoshima 890, Japan

[2] Institute of Earth Sciences, Faculty of Science, Kagoshima University
1-21-35 Korimoto, Kagoshima 890, Japan

[3] Kagoshima Prefectural Institute of Industrial Technology
1445-1 Hayato, Kagoshima 899-51, Japan

Abstract—Experimental alteration of obsidian in distilled-deionized water at 150°, 175°, 200°, and 225°C was studied. The alteration products were examined by X-ray powder diffraction, scanning electron microscopy, transmission electron microscopy (TEM), and energy dispersive X-ray analysis (EDX) to evaluate the formation process of clay minerals. The surface composition of obsidian before and after alteration was examined by X-ray photoelectron spectroscopy (XPS), and concentrations of released elements in solution were measured to elucidate alteration and dissolution processes. TEM clearly showed that allophane appeared as the first reaction product in each experiment. With increasing reaction length, noncrystalline straight fibrous material was formed in the aggregates of allophane particles as a metastable transitional phase, and tended to form curled or wavy bundles of fibers with longer reaction. The noncrystalline fibers were transformed into highly curled smectite exhibiting small circular forms less than 1.0 μm in diameter as reaction progressed. EDX confirmed that the smectite consisted mainly of Si, Al, and small amounts of Ca, K, and Fe. XPS revealed the formation of a dealkalized leached layer on the surface of obsidian during the reaction. The concentration of released elements suggested that nonstoichiometric dissolution proceeded during the reaction.

Key Words—Allophane, Dealkalized leached layer, Fibrous material, Nonstoichiometric dissolution, Obsidian, Smectite.

INTRODUCTION

Hydrous silicates are formed from volcanic glasses and rock-forming minerals as alteration products on the earth's surface. Smectite is one of the most abundant hydrous silicates produced by weathering processes and the early stages of diagenetic alteration and plays an important role in environmental processes as an ion-adsorption material. Therefore, the formation of smectite is a very important problem in clay mineralogy or environmental science. Experimental syntheses of smectites under high temperature conditions (> 200°C) have been extensively carried out to elucidate the formation mechanism of smectite during hydrothermal alteration and burial diagenesis (Mumpton and Roy, 1956; Koizumi and Roy, 1959; Levinson and Vian, 1966; Grandquist and Pollack, 1967; Komarneni and Breval, 1985; Imasuen *et al.*, 1989). However, syntheses under low temperature conditions (< 200°C) have been performed less frequently because 1) very long times are required to produce stable phases, and 2) amorphous metastable phases appear during the reaction that make thermodynamic evaluations difficult. Therefore, the formation of smectite under low temperature conditions is not well understood.

On the other hand, experimental studies on dissolution of nuclear waste glasses and soda-silica glasses under low temperature conditions have been exten-
sively carried out (Karkhanis *et al.*, 1981; Malow *et al.*, 1984; Murakami and Banba, 1984; Abrajano and Bates, 1986; Murakami *et al.*, 1989; Abrajano *et al.*, 1990; Banba *et al.*, 1990). According to these studies, various clay minerals including smectite could be formed from glasses by three processes: 1) transformation from thermodynamically metastable phase; 2) direct precipitation from leachant solution; and 3) development from a leached layer on the glass surface. For natural material, Tazaki *et al.* (1989) observed direct formation of clays from ordered domains in volcanic glass matrix using a high-resolution transmission electron microscopy (HRTEM).

The present study examined the experimental alteration of obsidian in aqueous solution at 150° to 225°C to evaluate smectite formation processes. Obsidian is one of the most abundant natural glasses having rhyolitic to dacitic chemical compositions. Most volcanic glasses consisting of tuffaceous sediments, pyroclastic flow deposits, and volcanic ash beds are also composed of similar compositions (Heiken and Wohletz, 1985; Wohletz, 1987). The results should be applicable to many natural alteration environments.

MATERIAL AND METHODS

Experimental alterations were performed using an obsidian from Mifune, Kagoshima City, Japan. K-Ar

Table 1. Experimental conditions and reaction products.

Run	Temp. (°C)	Duration	pH	Products
A-1	225	6 hr	7.7	Allophane, Fiber
A-2	225	1 day	7.8	Smectite, (As)
A-3	225	3 days	9.0	Smectite, (As)
A-4	225	5 days	9.2	Smectite, (As)
A-5	225	10 days	9.3	Smectite, (As)
A-6	225	30 days	9.4	Smectite, (As)
B-1	200	6 hr	7.5	Allophane, Fiber
B-2	200	1 day	7.7	Allophane, Fiber, (Halloysite)
B-3	200	3 days	8.8	Smectite, (As), (Halloysite)
B-4	200	5 days	9.2	Smectite, (As)
B-5	200	10 days	9.1	Smectite, (As)
B-6	200	30 days	8.9	Smectite, (As)
C-1	175	6 hr	7.1	Allophane
C-2	175	1 day	7.2	Allophane
C-3	175	3 days	7.9	Allophane, Fiber
C-4	175	5 days	7.9	Allophane, Fiber
C-5	175	10 days	8.3	Smectite, (Allophane), (As)
C-6	175	30 days	9.1	Smectite, (As)
D-1	150	6 hr	6.8	Allophane
D-2	150	1 day	6.8	Allophane
D-3	150	3 days	6.8	Allophane
D-4	150	5 days	8.2	Allophane, Fiber
D-5	150	10 days	8.7	Allophane, Fiber
D-6	150	30 days	8.6	Smectite, Mordenite, (Allophane)

( ) = trace product; Fiber = noncrystalline fibrous material; As = amorphous silica precipitate.

age for the material is 0.80 ± 0.08 Ma (Kaneoka and Suzuki, 1970). The chemical composition determined by electron probe microanalyzer is: 80.04% SiO_2, 12.27% Al_2O_3, 0.16% TiO_2, 0.84% FeO, 0.18% MgO, 1.10% CaO, 3.14% Na_2O, and 3.04% K_2O. This composition is slightly richer in SiO_2 than many obsidians. The Mifune obsidian is preferred because no impurities, such as feldspar inclusions, were detected by X-ray powder diffraction or optical microscopy. The obsidian was crushed in an agate mortar, and 50 to 100 mesh grains were separated by dry sieving. The selected grains contained small amounts of ultrafine particles, which were removed by ultrasonic cleaning in acetone at 40 W for 5 min more than five times. Then, the obsidian grains were air-dried at room temperature for 1 day.

In all experiments, 4.00 g of the starting material and 100 ml of distilled-deionized water were sealed in a Teflon bottle. Individual bottles were placed in a pressure vessel and kept at 150°, 175°, 200°, or 225°C for 6 hr or 1, 3, 5, 10, or 30 days. The pressure was the equilibrium vapor pressure at the corresponding temperature. After the hydrothermal treatment, the pressure vessels were quenched to room temperature, and the solids and solutions were separated by centrifugation. Small amounts of the solid (about 0.1 g) were used for scanning electron microscopy (SEM). The remainder was cleaned ultrasonically in acetone until no adhering reaction products could be detected by SEM and was used for X-ray photoelectron spectroscopy (XPS). The alteration products released by

cleaning were collected by centrifugation and were washed with distilled-deionized water. Portions of the suspensions were deposited on glass slides, carbon holders, and collodion films coated on copper grids and were air-dried at room temperature. These samples were used for X-ray powder diffraction (XRD), energy dispersive X-ray analysis (EDX), and transmission electron microscopy (TEM), respectively. The experimental conditions and reaction products are given in Table 1. The concentrations of soluble elements were measured by atomic absorption spectroscopy for Al, Mg, Fe, Na, K, and Ca, and by colorimetry for Si. SEM was carried out with a JEOL JSM-25SII scanning electron microscope operated at an accelerating voltage of 25 kV. XRD profiles of the products were obtained from samples deposited on glass slides with a RI-GAKU RU-200 diffractometer (CuKα radiation, 30 kV, 100 mA) equipped with a graphite monochrometer. EDX was performed with a JEOL JSM-840 scanning electron microscope equipped with EDX facilities using carbon-coated samples mounted on carbon holders that were free from contamination. TEM was carried out with a HITACHI H-700H transmission electron microscope operated at an accelerating voltage of 200 kV using samples deposited on collodion films. XPS was done with a SHIMAZU ESCA-1000 instrument using samples mounted on a carbon holder. The MgKα radiation (8 kV, 20 mA) was used for X-ray source. Calibration of the XPS binding energy was obtained by using the C_{1s} signal of carbon at 284.6 eV.
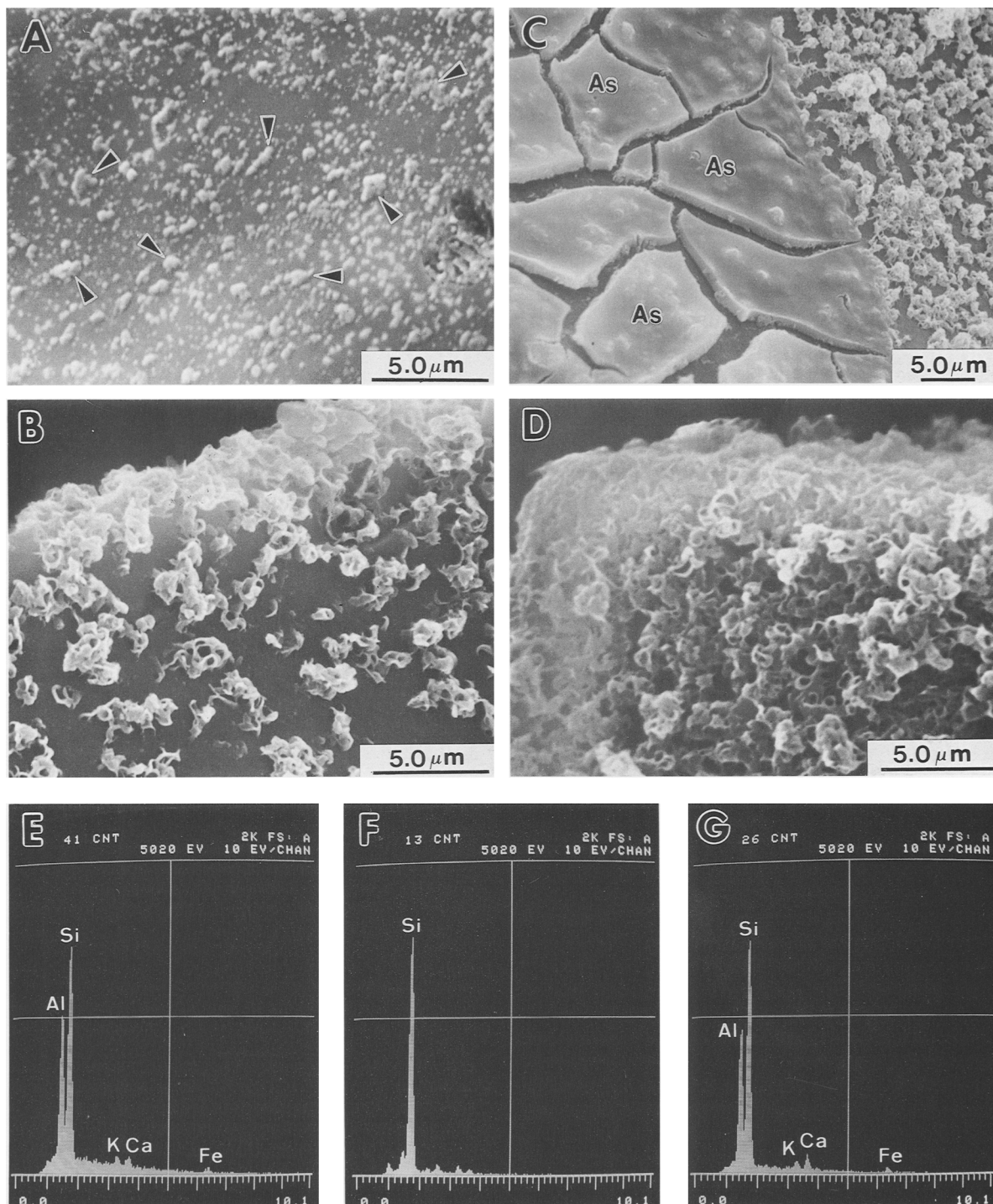
Figure 1. Scanning electron micrographs of reaction products formed by experimental alteration at 200°C for A) 6 hr, B) 1 day, C) 3 days, and D) 5 days. Also, energy dispersive X-ray spectra of E) aggregate of fine material in the 6-hr product, F) amorphous silica precipitate in the 3-day product, and G) flaky material in the 3-day product. Arrows on A indicate aggregates of allophane. As on C represents amorphous silica precipitate.
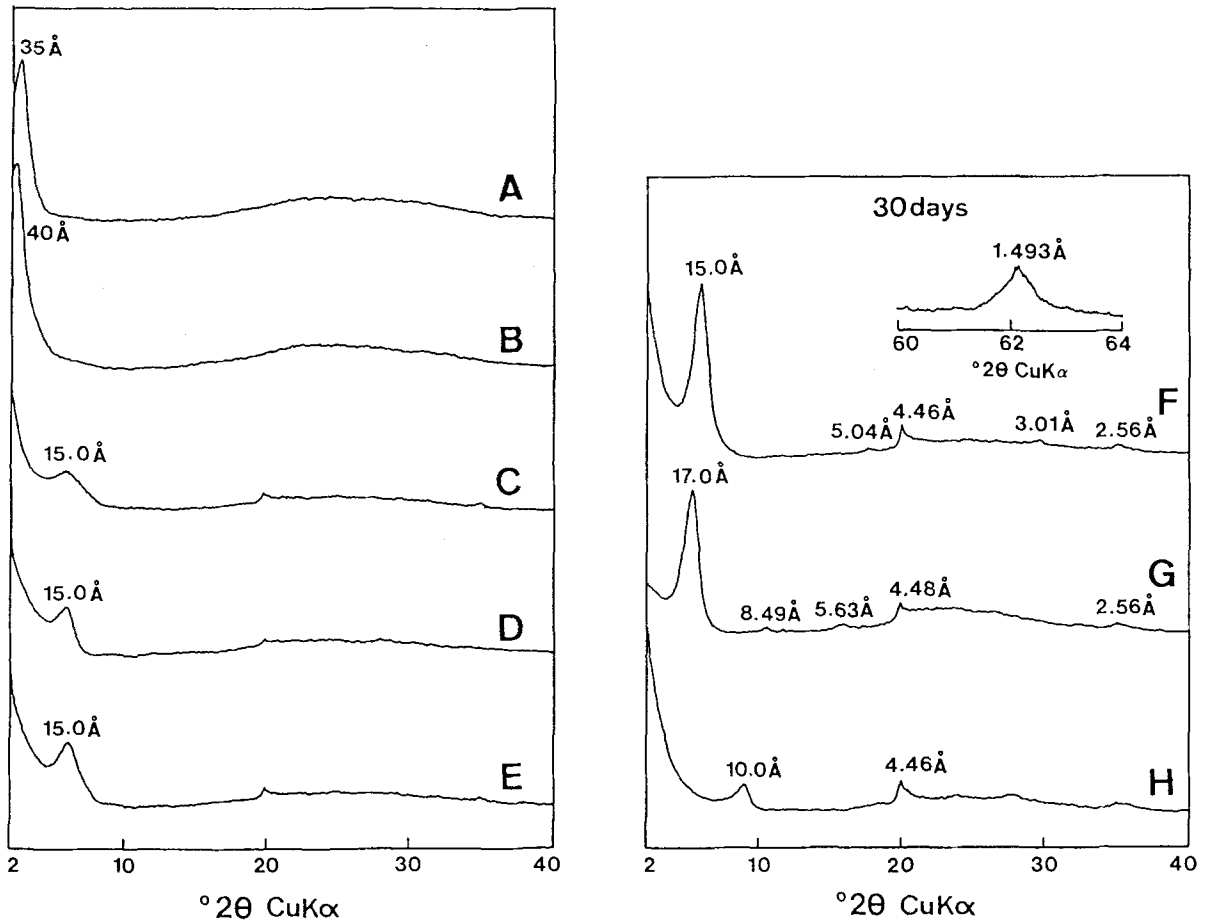
Figure 2.   X-ray powder diffraction profiles of reaction products formed by experimental alteration at 200°C for various periods of duration. The labels A to E represent 6-hr, 1-, 3-, 5-, and 10-day products, respectively. The labels F to H signify products at 200°C for 30 days under natural state, solvated with ethylene glycol, and heated at 400°C for 1 hr, respectively.

RESULTS

Formation process of clay minerals

For the 200°C experiment, small aggregates of al-lophane-like amorphous material less than 1.0 μm in diameter appeared initially on the surface of obsidian after 6 hr (Figure 1A). XRD of the material exhibited small-angle scattering of allophane particles at 35 Å (Figure 2A). EDX indicated that the material consisted mainly of Si and Al, and small amounts of Ca and K (Figure 1E). TEM showed aggregates of allophane par-ticles and fibrous materials elongated in a straight line approximately 0.1 to 0.2 μm in length with less than 0.005 μm in width (Figure 3A). Electron diffraction patterns of the fibers displayed a diffuse halo implying noncrystalline structure.

The aggregates changed morphologically to flaky ma-terial after 1 day (Figure 1B). The flaky material showed similar EDX spectrum (not shown) to that of 6 hr product. XRD exhibited no significant reflection of crystalline material except for small-angle scattering at

40 Å (Figure 2B). The aggregates of allophane particles were still preserved in this product; however, the non-crystalline fibers tended to be curled or waved bundles of fibers and became greater to approximately 1.0 μm in maximum length (Figure 3B). The electron diffrac-tion pattern with a diffuse halo confirmed that these fibers were also noncrystalline.

After 3 days, a new reaction product of amorphous silica precipitated on the surface of obsidian overlaying the adhering flaky material. The amorphous silica pre-cipitates showed thin platy habit less than 2.0 μm in thickness and smooth surface with cracks (Figure 1C). EDX confirmed that the precipitates consisted mainly of Si and very small amounts of Al and Na (Figure 1F). The flaky material gave a weak 15.0 Å reflection, in-dicating that the material may be smectite (Figure 2C). TEM showed that the smectite exhibited curled fibrous habit or roughly circular texture as shown in Kawano and Tomita (1992). Electron diffraction displayed dif-fuse ring patterns, suggesting poorly crystalline struc-ture. The d(060) spacing is 1.493 Å, indicating dioc-
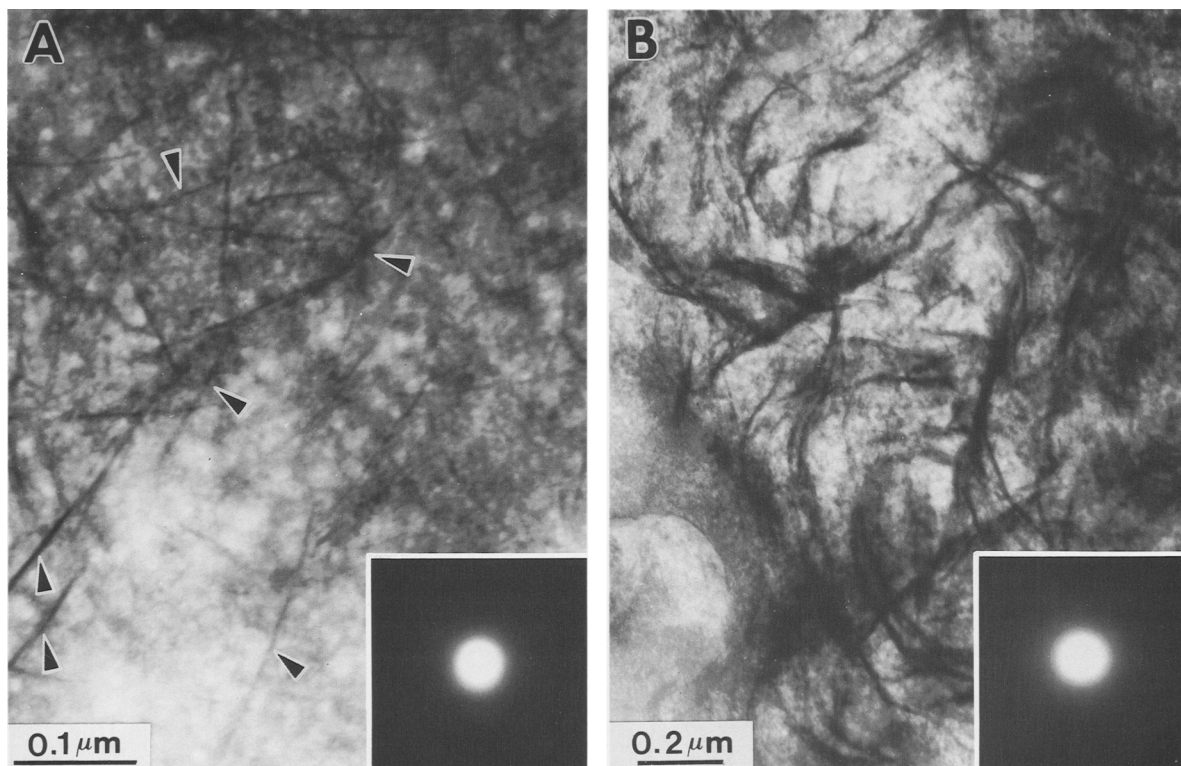
Figure 3.   Transmission electron micrographs of reaction products formed by experimental alteration at 200°C for A) 6 hr and B) 1 day. Arrows on A indicate straight fibers.

tahedral nature. EDX showed that the material consisted mainly of Si, Al, and small amounts of Fe, Ca, and K (Figure 1G).

The surface of obsidian was completely covered by flaky material (Figure 1D) and partly by amorphous silica precipitates after 5 days. XRD of the flaky material showed 15.0 Å reflection (Figure 2D), which shifted to 17.0 and 10.0 Å after ethylene glycol solvation and heating at 400°C for 1 hr, respectively. The d-value of (060) reflection is 1.493 Å; thus, the flaky material can be identified as dioctahedral smectite. TEM showed that the smectite exhibited circular texture of fibers that curled inward, forming small circles less than 1.0 μm in diameter (Figure 4A). Most of the fibers gave electron diffraction of ring patterns at 4.50, 2.62, 1.56, and 1.28 Å. HRTEM of a randomly oriented fiber showed 10.0 Å parallel lattice images that coincided with the basal spacing of dehydrated smectite (Figure 4B). EDX indicated that the smectite consisted mainly of Si, Al, and very small amounts of Fe, Ca, and K (Figure 4C). The 10- and 30-day products also gave characteristic XRD profiles of dioctahedral smectite (Figure 2) and electron diffraction of ring patterns. The circular habit of smectite as shown in Figure 4A has also been preserved well in these products.

For the 150°C products, similar developments of

alteration products were observed by TEM. Noncrystalline fibers appeared in the aggregates of allophane particles after 5 days. The fibrous materials increased as reaction progressed, and were finally transformed into circular smectite after 30 days. For the 175°C experiment, allophane appeared as first alteration product within 6 hr. Noncrystalline fibers were produced by 3-day reaction and were transformed into circular smectite after 10 days. For the 225° C experiment, noncrystalline straight fibrous materials were formed within 6 hr and were transformed rapidly into circular smectite during 1-day reaction. These circular smectites exhibited similar XRD characteristics and EDX spectra to those of 200°C product.

Alteration of the obsidian surface

During the reaction process between obsidian and distilled-deionized water, tiny elongated submicrometer- to micrometer-sized etch pits (Figure 5) appeared on the obsidian surface. The etch pits may be developed at mechanically strained parts by grinding and increased as reaction progresses. Figure 6 shows XPS spectra of obsidian before and after alteration at 200°C for various periods of duration, in which electron lines of Ca_{2p}, C_{1s}, K_{2s}, Na_{KLL}, Si_{2s}, Al_{2s}, Si_{2p}, Al_{2p}, and O_{2s} can be clearly observed. No significant changes
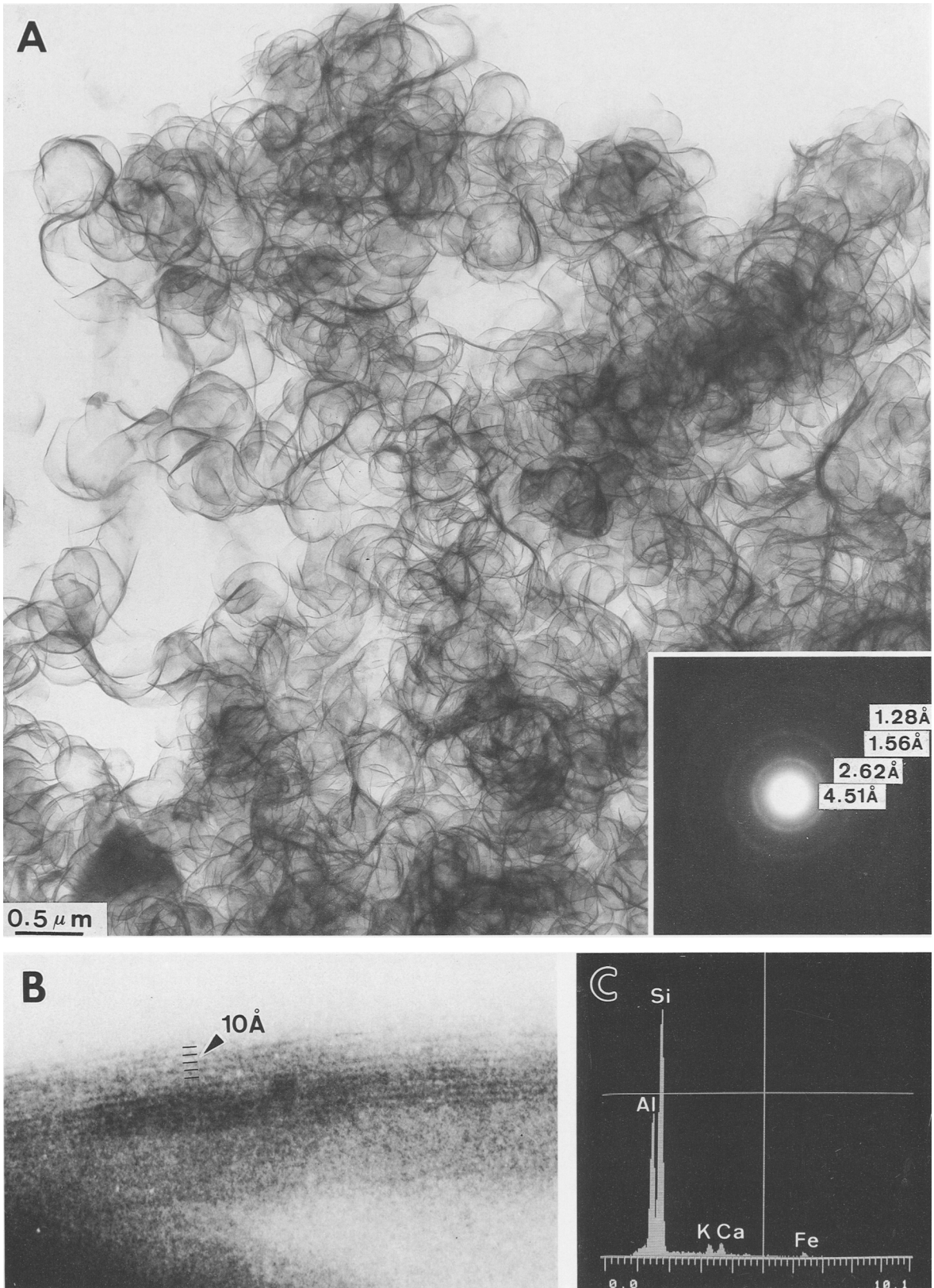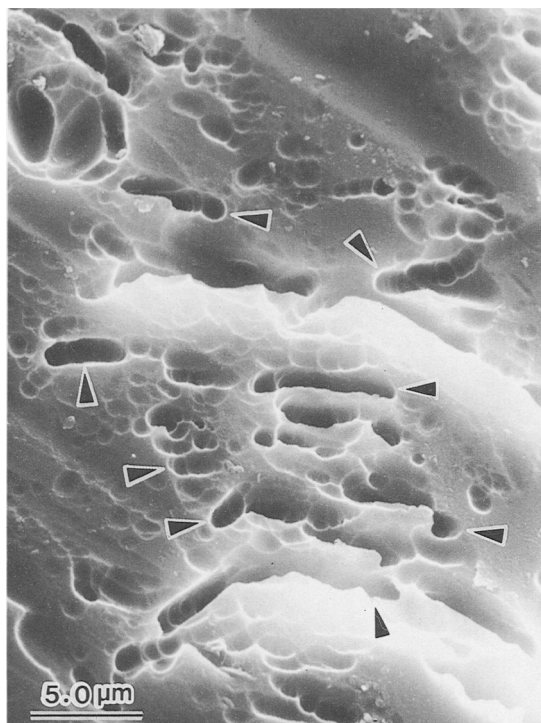
Figure 5. Scanning electron micrograph of the surface of obsidian after alteration at 200°C for 5 days. Arrows indicate etch pits.

Figure 6. X-ray photoelectron spectra of obsidian before and after alteration at 200°C for various periods of duration.

in intensities and binding energies of Si_{2s}, Al_{2s}, Si_{2p}, and Al_{2p} were recognized during reaction; however, Na_{KLL} Auger and K_{2s} electron lines were weakened as the reaction progressed. The residual obsidian used in 150°, 175°, and 225°C experiments also showed alkali depletion relative to Si. These results suggest that selective leaching of alkali ions has proceeded and a dealkalized leached layer has been progressively produced on the obsidian surface (Doremus, 1975; Lanford *et al.,* 1979; Houser *et al.,* 1980; Smets and Lommen, 1982). TEM showed formation of a very thin leached layer less than 0.1 μm in thickness on the obsidian surface in all the experiments (Figure 7). The leached layers faithfully followed the original glass surface with shape boundary and were noncrystalline for electron diffraction.

Chemistry of solutions

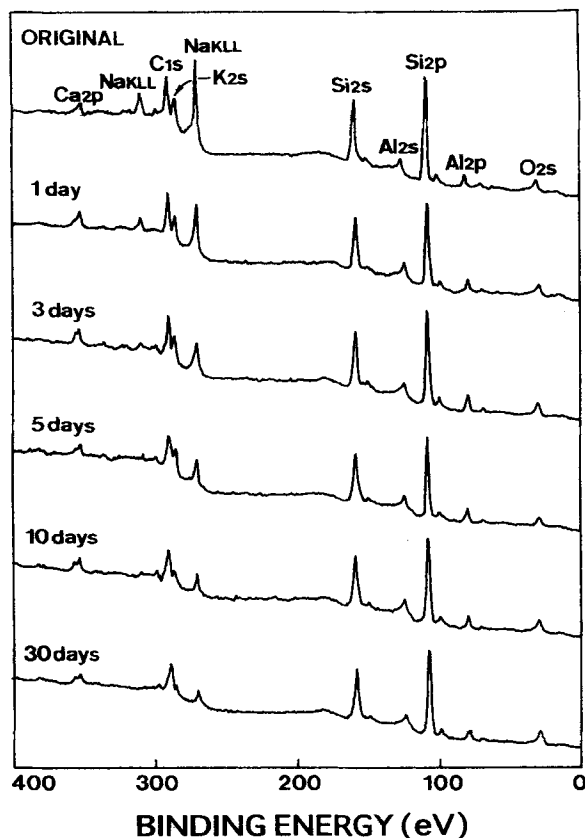Reaction of the obsidian with distilled-deionized water resulted in changes in composition and pH of the solution. Figure 8 shows concentrations of elements released from dissolution of the obsidian during experimental alterations. Fe values were below detection limit of the instrument (0.01 ppm). The concentrations of released elements increased rapidly during the initial stage of reaction within 10 days. After this, the rates of changes in Si, Al, Na, and K decreased and the concentrations of Ca and Mg decreased slowly. Figure 9 shows variations of Na/Si and Si/Al molar ratios in solutions as a function of the square root of time. Arrows on this figure represent Na/Si and Si/Al molar ratios of the original obsidian. The Na/Si ratios changed considerably differently from each other at the beginning of the reaction: The Na/Si ratios of the solutions at 225°C experiments increased rapidly but those of the 150°C experiments decreased. This observation is probably due to increases in pH values with temperature, which stimulate the leaching rate of Si in high

←

Figure 4. Transmission electron micrograph and electron diffraction pattern of A) reaction product formed by experimental alteration at 200°C for 5 days, B) high-resolution transmission electron micrograph, and C) energy dispersive X-ray spectrum of the product.
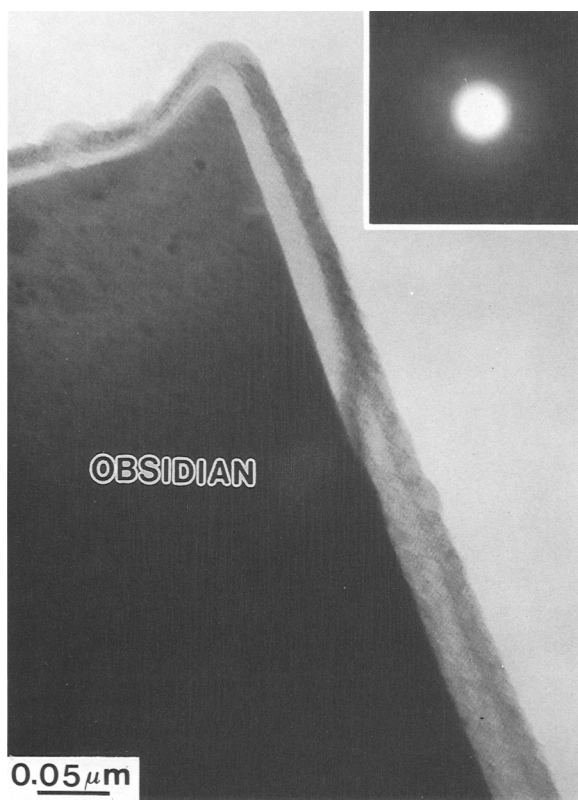
Figure 7. Transmission electron micrograph and electron diffraction pattern of a leached layer on the obsidian surface produced by experimental alteration at 200°C for 1 day.

temperature experiments (Barkatt *et al.,* 1986). However, the rates of change tended to decrease during the reaction and kept apparently higher values than those of the original obsidian. The results suggest that nonstoichiometric dissolution takes place in the early dissolution stage, producing a dealkalized protective layer on alkali leaching (Berner, 1978). This protective layer reduces the rate of alkali dissolution, which leads to stabilized Na/Si ratios in solutions. On the other hand, the Si/Al ratios in the 225°, 200°, and 175°C experiments increased progressively, and ratios at 150°C were slightly lower than those of the others. This is probably due to decreases in the consumption of released Al for secondary products of 150°C experiments.

DISCUSSION

TEM revealed the formation process of smectite during experimental alteration of obsidian in distilled-deionized water in 150° to 225°C experiments as in the following three steps:

1) Allophane appeared as the first alteration product.
2) Noncrystalline straight fibrous materials were formed in the aggregates of allophane particles as a metastable transitional phase and tended to form curled or wavy bundles of fibers as reaction progressed.
3) The fibrous transitional materials were transformed into circular-shaped smectite having a beidellitic composition.

It is well known that allophane is a noncrystalline aluminum-silicate having short-range ordered structure (van Olphen, 1971). Such materials are widely distributed on the earth's surface as important constituents of soils developed from volcanic ashes and pumices (Allen and Hajek, 1989; Parfitt and Kimble, 1989; Wada, 1989), early weathering products of feldspar and rocks (Patterson, 1964; Tazaki, 1978; Eswaran, 1979), and precipitates in river stream beds (Wells *et al.,* 1977). Wada *et al.* (1979) synthesized allophane from solutions containing Si and Al by adding NaOH and maintaining at 95°–100°C. They found that allophane was produced in the solution with Si/Al ratios of 0.5 to 4.0 and a pH range of 3.3 to 7.2. The formation mechanism of allophane has not been clarified in detail; however, its common occurrence in nature and easy formation in the laboratory suggest that the material may be produced by reorganization of aluminum-silicate leached from volcanic glasses and various minerals under wide ranges of Si/Al ratios and pH conditions. In the present study, allophane was formed in the solution having an Si/Al ratio of 3.5 to 6.3 (Figure 9B) and pH range of 6.8 to 8.6 (Table 1). On the basis of field observation, two series of transformation sequences of clay minerals from volcanic glasses have been considered: 1) volcanic glass → allophane → halloysite; and 2) volcanic glass → allophane → smectite. However, there is no report concerning direct observation of transitional process of these clay minerals in nature. The formation process of clay minerals observed in this study coincided with Sequence 2, and noncrystalline transitional materials from allophane to smectite were clearly visualized by TEM. The transitional materials exhibited noncrystalline straight fibers initially and tended to form curled or wavy bundles of fibers later (Figure 3). Finally, the fibers were transformed into circular smectite (Figure 4).

This experimental study was performed at temperatures between 150° and 225°C, and concentrations of cations in solutions were relatively high. For the natural weathering, chemical reactions proceed generally at low temperature and low cation concentrations. Therefore, the present results can not be directly applied to the weathering processes. However, similar fibrous materials have been reported as precursors of clays produced by early weathering process (Tazaki, 1986; Tazaki and Fyfe, 1985, 1987a, 1987b; Tazaki *et al.,* 1989). Consequently, the formation process of smectite observed in this study seems to be one of the possible processes occurring in nature.
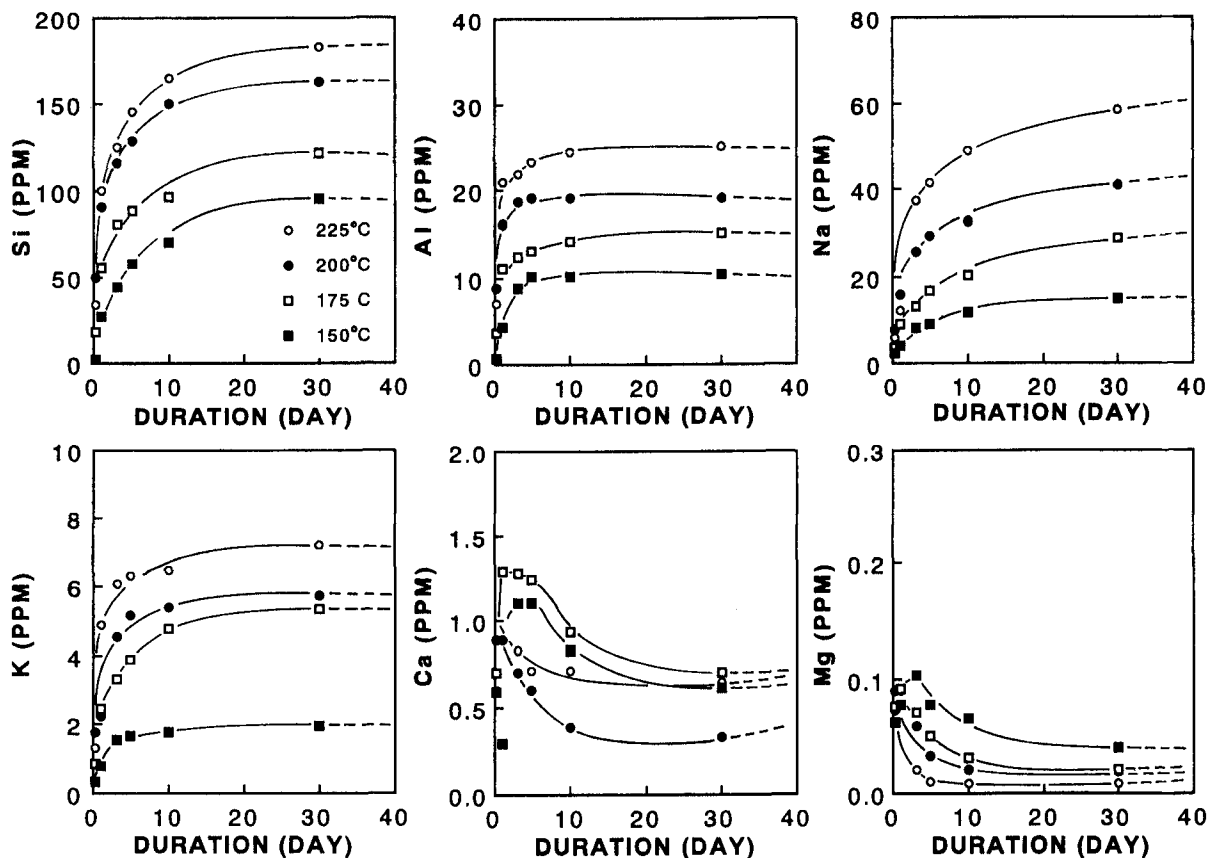
Figure 8.　Concentrations of elements released from obsidian in solutions. The symbols ■, □, ●, and ○ signify the 150°, 175°, 200°, and 225°C experiments, respectively.
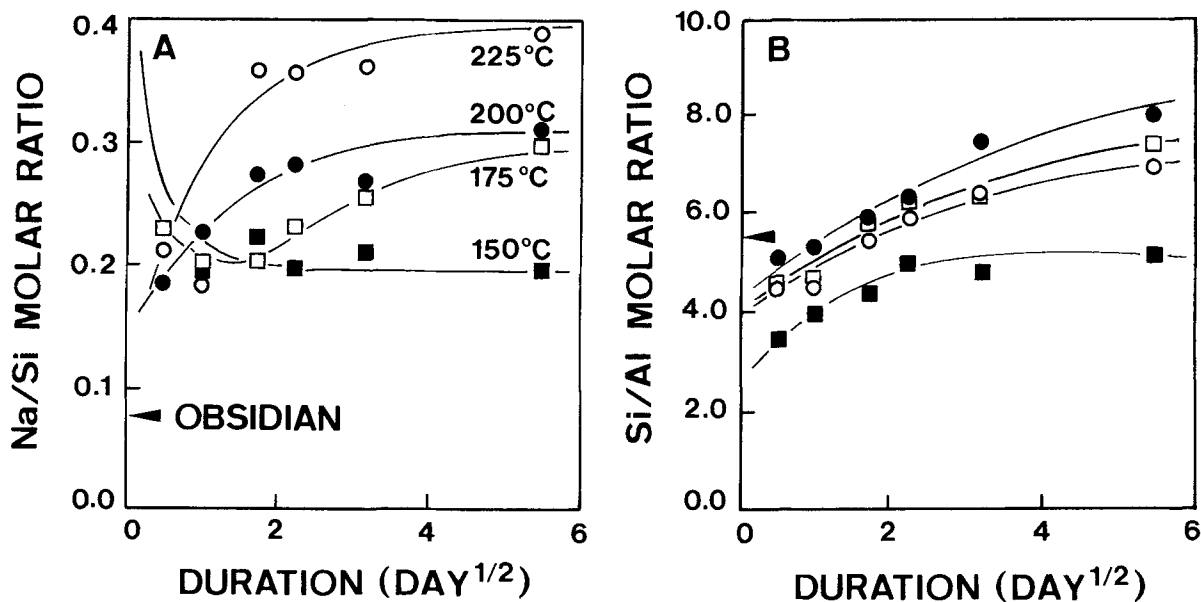

Figure 9.　Variations of A) Na/Si and B) Si/Al molar ratios in solutions as a function of the square root of time. The symbols ■, □, ●, and ○ signify the 150°, 175°, 200°, and 225°C experiments, respectively. Arrows in Figures A and B represent the Na/Si and Si/Al molar ratios of the original obsidian, respectively.

ACKNOWLEDGMENTS

REFERENCES

Abrajano Jr., T. A. and Bates, J. K. (1986) Transport and reaction kinetics at the glass: Solution interface region: Results of repository-oriented leaching experiments: in *Scientific Basis for Nuclear Waste Management X*, J. K. Bates and W. B. Seefeldt, eds., Material Research Society, Pittsburgh, 533–546.

Abrajano, T. A., Bates, J. K., Woodland, A. B., Bradley, J. P., and Bourcier, W. L. (1990) Secondary phase formation during nuclear waste-glass dissolution: *Clays & Clay Minerals* **38**, 537–548.

Allen, B. L. and Hajek, B. F. (1989) Mineral occurrence in soil environments: in *Minerals in Soil Environments*, J. B. Dixon and S. B. Weed, eds., Soil Science Society, Wisconsin, 199–278.

Banba, T., Murakami, T., and Isobe, H. (1990) Growth rate of alteration layer and elemental losses during leaching of borosilicate nuclear glass: in *Scientific Basis for Nuclear Waste Management XIII*, V. M. Oversby and P. W. Brown, eds., Materials Research Society, Pittsburgh, 363–370.

Barkatt, A., Gibson, B. C., Macedo, P. B., Montrose, C. J., Sousanpour, W., Barkatt, A., Boroomand, M., Rogers, V., and Penafiel, M. (1986) Mechanisms of defense waste glass dissolution: *Nuclear Tech.* **73**, 140–164.

Berner, R. A. (1978) Rate control of mineral dissolution under earth surface conditions: *Am. J. Sci.* **278**, 1235–1252.

Doremus, R. H. (1975) Interdiffusion of hydrogen and alkali ions in a glass surface: *J. Non-Cryst. Solids* **19**, 137–144.

Eswaran, H. (1979) The alteration of plagioclases and augites under differing pedo-environmental conditions: *J. Soil Sci.* **30**, 547–555.

Grandquist, W. T. and Pollack, S. S. (1967) Clay mineral synthesis. II—A randomly interstratified aluminian montmorillonoid: *Amer. Mineral.* **52**, 212–226.

Heiken, G. and Wohletz, K. (1985) *Volcanic Ash:* University of California Press, Berkeley, 246 pp.

Houser, C. A., Herman, J. S., Tsong, I. S. T., White, W. B., and Lanford, W. A. (1980) Sodium-hydrogen interdiffusion in sodium silicate glasses: *J. Non-Cryst. Solids* **41**, 89–98.

Imasuen, O. I., Tazaki, K., Fyfe, W. S., and Kohyama, N. (1989) Experimental transformations of kaolinite to smectite: *Appl. Clay Sci.* **4**, 27–41.

Kaneoka, I. and Suzuki, M. (1970) K-Ar and fission track ages of some obsidians from Japan: *Geol. Soc. Japan* **76**, 309–313.

Karkhanis, S. N., Melling, P. J., Fyfe, W. S., and Bancroft, G. M. (1981) Stable product low leach glasses: in *Scientific Basis for Nuclear Waste Management, Vol. 3*, J. G. Moore, ed., Plenum Press, New York, 115–122.

Kawano, M. and Tomita, K. (1992) Formation of allophane and beidellite during hydrothermal alteration of volcanic glass below 200°C: *Clays & Clay Minerals* **40**, 666–674.

Koizumi, M. and Roy, R. (1959) Synthetic montmorillonoids with variable exchange capacity: *Amer. Miner.* **44**, 788–805.

Komarneni, S. and Breval, E. (1985) Characterization of smectites synthesized from zeolites and mechanism of smectite synthesis: *Clay Miner.* **20**, 181–188.

Lanford, W. A., Davis, K., Lamarche, P., Laursen, T., and Groleau, R. (1979) Hydration of soda-lime glass: *J. Non-Cryst. Solids* **33**, 249–266.

Levinson, A. A. and Vian, R. W. (1966) The hydrothermal synthesis of montmorillonite group minerals from kaolinite, quartz and various carbonates: *Amer. Mineral.* **51**, 495–498.

Malow, G., Lutze, W., and Ewing, R. C. (1984) Alteration effects and leach rates of basaltic glasses: Implication for the long-term stability of nuclear waste form borosilicate glasses: *J. Non-Cryst. Solids* **67**, 305–321.

Mumpton, F. A. and Roy, R. (1956) The influence of ionic substitution on the hydrothermal stability of montmorillonoids: *Clays & Clay Minerals* **3**, 337–339.

Murakami, T. and Banba, T. (1984) The leaching behavior of a glass waste form-part I: The characteristics of surface layers: *Nuclear Tech.* **67**, 419–428.

Murakami, T., Banba, T., Jercinovic, M. J., and Ewing, R. C. (1989) Formation and evolution of alteration layers on borosilicate and basalt glasses: Initial stage: in *Scientific Basis for Nuclear Waste Management XII*, W. Lutze and R. C. Ewing, eds., Materials Research Society, Pittsburgh, 65–72.

Parfitt, R. L. and Kimble, J. M. (1989) Conditions for formation of allophane in soils: *Soil Sci. Soc. Am. J.* **53**, 971–977.

Patterson, S. H. (1964) Halloysitic underclay and amorphous inorganic matter in Hawaii: in *Clays and Clay Minerals, Proc. 12th Nat. Conf., Atlanta, Georgia, 1963*, W. F. Brindley, ed., Pergamon Press, New York, 153–172.

Smets, B. M. and Lommen, T. P. A. (1982) The leaching of sodium aluminosilicate glasses studied by secondary ion mass spectrometry: *Phys. Chem. Glasses* **23**, 83–87.

Tazaki, K. (1978) Micromorphology of plagioclase surface at incipient stage of weathering: *Earth Science (Chikyu Kagaku)* **32**, 58–62 (in Japanese).

Tazaki, K. (1986) Observation of primitive clay precursors during microcline weathering: *Contrib. Mineral. Petrol.* **62**, 86–88.

Tazaki, K. and Fyfe, W. S. (1985) Discovery of "primitive clay precursors" on alkali-feldspar: *Earth Science (Chikyu Kagaku)* **39**, 443–445 (in Japanese).

Tazaki, K. and Fyfe, W. S. (1987a) Formation of primitive clay precursors on K-feldspar under extreme leaching conditions: in *Proc. Inter. Clay Conf., Denver, 1985*, L. G. Schultz, H. van Olphen, and F. A. Mumpton, eds., The Clay Mineralogical Society, Bloomington, Indiana, 53–58.

Tazaki, K. and Fyfe, W. S. (1987b) Primitive clay precursors formed on feldspar: *Canadian J. Earth Sciences* **24**, 506–527.

Tazaki, K., Fyfe, W. S., and van der Gaast, S. J. (1989) Growth of clay minerals in natural and synthetic glasses: *Clays & Clay Minerals* **37**, 348–354.

Van Olphen, H. (1971) Amorphous clay materials: *Science* **171**, 90–91.

Wada, K. (1989) Allophane and imogolite: in *Minerals in Soil Environments*, J. B. Dixon and S. W. Weed, eds., Soil Science Society, Wisconsin, 1051–1088.

Wada, S.-I., Eto, A., and Wada, K. (1979) Synthetic allophane and imogolite: *J. Soil Sci.* **30**, 347–355.

Wells, N., Childs, C. W., and Downes, C. J. (1977) Silica spring, Tongariro National Park, New Zealand—Analysis of the spring water and characterization of the alumino-silicate deposit: *Geochim. Cosmochim. Acta* **41,** 1498–1506.

Wohletz, K. H. (1987) Chemical and textural surface features of pyroclasts from hydrovolcanic eruption sequences: in *Clastic Particles,* J. R. Marshall, ed., Van Nostrand Reinhold Company, New York, 79–97.